



Monosynaptic Retrograde Tracing From Prelimbic Neuron Subpopulations Projecting to Either Nucleus Accumbens Core or Rostromedial Tegmental Nucleus

Adelis M. Cruz¹, Tabitha H. Kim¹ and Rachel J. Smith^{1,2*}

¹Department of Psychological and Brain Sciences, Texas A&M University, College Station, TX, United States, ²Institute for Neuroscience, Texas A&M University, College Station, TX, United States

OPEN ACCESS

Edited by:

Sam Adler Golden,
University of Washington,
United States

Reviewed by:

Ryan LaLumiere,
The University of Iowa, United States
Jacqueline F. McGinty,
Medical University of South Carolina,
United States

Nathan James Marchant,
VU University Medical Center,
Netherlands

Marco Venniro,
University of Maryland, Baltimore,
United States

*Correspondence:

Rachel J. Smith
rachelsmith@tamu.edu

Received: 09 December 2020

Accepted: 01 February 2021

Published: 25 February 2021

Citation:

Cruz AM, Kim TH and Smith RJ (2021) Monosynaptic Retrograde Tracing From Prelimbic Neuron Subpopulations Projecting to Either Nucleus Accumbens Core or Rostromedial Tegmental Nucleus. *Front. Neural Circuits* 15:639733. doi: 10.3389/fncir.2021.639733

The prelimbic (PL) region of the medial prefrontal cortex (mPFC) has been implicated in both driving and suppressing motivated behaviors, including cocaine-seeking in rats. These seemingly opposing functions may be mediated by different efferent targets of PL projections, such as the nucleus accumbens (NAc) core and rostromedial tegmental nucleus (RMTg), which have contrasting roles in reward-seeking behaviors. We sought to characterize the anatomical connectivity differences between PL neurons projecting to NAc core and RMTg. We used conventional retrograde tracers to reveal distinct subpopulations of PL neurons projecting to NAc core vs. RMTg in rats, with very little overlap. To examine potential differences in input specificity for these two PL subpopulations, we then used Cre-dependent rabies virus (EnvA-RV-EGFP) as a monosynaptic retrograde tracer and targeted specific PL neurons via injections of retrograde CAV2-Cre in either NAc core or RMTg. We observed a similar catalog of cortical, thalamic, and limbic afferents for both NAc- and RMTg-projecting populations, with the primary source of afferent information arising from neighboring prefrontal neurons in ipsilateral PL and infralimbic cortex (IL). However, when the two subpopulations were directly compared, we found that RMTg-projecting PL neurons received a greater proportion of input from ipsilateral PL and IL, whereas NAc-projecting PL neurons received a greater proportion of input from most other cortical areas, mediadorsal thalamic nucleus, and several other subcortical areas. NAc-projecting PL neurons also received a greater proportion of contralateral cortical input. Our findings reveal that PL subpopulations differ not only in their efferent target but also in the input specificity from afferent structures. These differences in connectivity are likely to be critical to functional differences of PL subpopulations.

Keywords: rabies, addiction, reinstatement, RMTg, medial prefrontal cortex (mPFC)

INTRODUCTION

The prelimbic (PL) region of the medial prefrontal cortex (mPFC) plays roles in both driving and suppressing motivated behaviors, including drug-seeking and conditioned fear (Moorman et al., 2015; Gourley and Taylor, 2016). Opposing behavioral functions for PL may be mediated by distinct efferent projections. This is supported by previous work demonstrating bidirectional behavioral effects after optogenetic stimulation of distinct PL projection pathways, including PL projections to lateral habenula vs. dorsal raphe in a forced swim task (Warden et al., 2012), nucleus accumbens (NAc) vs. basolateral amygdala (BLA) in an active avoidance task (Diehl et al., 2020), and NAc vs. paraventricular nucleus of the thalamus during cue-induced reward-seeking (Otis et al., 2017). Additionally, whereas PL projections to NAc core have been shown to drive cue-induced reinstatement of cocaine-seeking (McFarland et al., 2003; Stefanik et al., 2013, 2016; McGlinchey et al., 2016; James et al., 2018), we recently showed that PL projections to the rostromedial tegmental nucleus (RMTg) play a suppressive role in cue-induced reinstatement (Cruz et al., 2020).

Here, we sought to characterize anatomical connectivity differences between PL neurons projecting to NAc core and RMTg, given that these two efferent targets often have opposing influences on reward-seeking behavior. The NAc core is critically involved in driving motivated behavior and action initiation, particularly when guided by incentive stimuli (Du Hoffmann and Nicola, 2014; Floresco, 2015; Hamid et al., 2016; Syed et al., 2016; Mohebi et al., 2019; Sicre et al., 2019). Conversely, the RMTg, or tail of the ventral tegmental area (tVTA), is involved in behavioral inhibition and aversive valence encoding, *via* its inhibitory influence on dopamine neurons in the ventral tegmental area (Jhou et al., 2009a,b, 2013; Kaufling et al., 2009, 2010; Balcita-Pedicino et al., 2011; Barrot et al., 2012; Bourdy et al., 2014; Vento et al., 2017; Li et al., 2019; Smith et al., 2019). Previous work has demonstrated that mPFC projections to a variety of brain structures typically arise from different subpopulations of mPFC neurons (Akintunde and Buxton, 1992; Pinto and Sesack, 2000; Gabbott et al., 2005). Therefore, we hypothesized that distinct subpopulations of PL neurons project to NAc core vs. RMTg, and we sought to investigate connectivity differences for these subpopulations, as differences in input/output specificity are likely to be critical to their functional differences.

Using conventional retrograde tracers, we show that PL neurons projecting to NAc core and RMTg are markedly separate, forming two largely distinct sublayers of pyramidal cells in rats (**Figure 1**). Therefore, we investigated these two PL projection pathways in terms of afferent connectivity, considering that input specificity might influence differential recruitment of these populations during behavior. We used Cre-dependent rabies (EnvA-RV-EGFP) as a monosynaptic retrograde tracer to determine direct afferents to the two different PL projection neuron subpopulations (Wickersham et al., 2007a,b, 2010; Callaway, 2008; Wall et al., 2010, 2013; Watabe-Uchida et al., 2012). Cre was expressed specifically in RMTg- or NAc-projecting neurons using retrograde CAV2-Cre

microinjected into the efferent target (RMTg or NAc), followed by microinjection of AAV helper viruses and EnVA-RV-EGFP into PL. Our results revealed that PL neurons projecting to either NAc core or RMTg receive input from similar afferents, but differ in the proportions of input arising from these afferents.

MATERIALS AND METHODS

Animals

Male Sprague Dawley rats (initial weight 250–300 g; Charles River, Raleigh, NC, USA) were single-housed under a 12-h reverse light/dark cycle (ZT0 = 19:00) and had access to food and water *ad libitum*. Animals were housed in a temperature- and humidity-controlled animal facility with AAALAC accreditation. All experiments were approved by the Institutional Animal Care and Use Committee at Texas A&M University and conducted according to specifications of the National Institutes of Health as outlined in the Guide for the Care and Use of Laboratory Animals.

Viruses

The transduction and monosynaptic spread of glycoprotein (G)-deleted rabies virus (RV) with EnvA pseudotyping (EnvA-RV-EGFP) is limited to neurons expressing TVA receptor and rabies glycoprotein (RG) in a Cre-dependent manner (Wickersham et al., 2007a,b; Watabe-Uchida et al., 2012). We targeted specific PL neurons by injecting either NAc core or RMTg with retrograde Cre-expressing virus (CAV2-Cre) and injecting PL with Cre-dependent helper AAV viruses (TVA and RG) and EnvA-RV-EGFP.

EnvA-RV-EGFP (titer of 4.3×10^{8}) was provided by Ed Callaway *via* the Gene Transfer, Targeting, and Therapeutics Facility at the Salk Institute (Wickersham et al., 2007a). AAV-TVA (AAV1-EF1a-FLEX-TVAmCherry, a titer of 4×10^{12}) and AAV-RG (AAV1-CA-FLEX-RG, a titer of 4×10^{12}) were obtained through the viral vector core at the University of North Carolina (developed by Watabe-Uchida et al., 2012). CAV2-Cre (CAV2-CMV-Cre recombinase) was provided by Eric J. Kremer at the Institut de Génétique Moléculaire de Montpellier (Kremer et al., 2000). We diluted CAV2-Cre 1:10 in 10% glycerol in PBS for a final titer of 10.3×10^{11} ppml, based on preliminary experiments indicating cell toxicity at higher titers. All viral procedures were approved by the Institutional Biosafety Committee at Texas A&M University and conducted according to specifications of the National Institutes of Health.

Stereotaxic Surgery

Rats were anesthetized with vaporized isoflurane (induced at 5%, maintained at 1–2%), given the analgesic ketoprofen (2 mg/kg, s.c.), and placed in a stereotaxic frame (Kopf, Tujunga, CA, USA). A skin incision was made over the skull and holes were drilled in the skull over the target sites. Intracranial injections were made using a pulled glass micropipette and Nanoject 2010 injector (World Precision Instruments, Sarasota, FL, USA). After the injection, the pipette was slowly raised from the brain and the skin was stapled closed.

For conventional retrograde tracing, rats were given unilateral microinjections of 100 nl of 2% Fluoro-Gold (FG, Fluorochrome, Denver, CO, USA) into unilateral NAc core (AP +1.8, ML +2.6, DV -7.3 from bregma, 6°) and 100 nl of 0.2% cholera toxin subunit b (CTB, List Biological Laboratories, Campbell, CA, USA) into RMTg (AP -7.2, ML +1.9, DV -7.6 from dura, 10°). FG was used only in NAc because it tended to cause toxicity in RMTg, evident by circling of animals after unilateral injection. Rats were sacrificed at least 1 week after injections.

For monosynaptic retrograde tracing, rats were given two surgeries. During the first stereotaxic surgery, CAV2-Cre (1,000 nl) plus biotin dextran (10 K MW, 0.2% final volume, for visualization of injection site) was injected unilaterally into either NAc core (AP +1.8, ML +2.6, DV -7.3 from bregma, 6°) or RMTg (AP -7.2, ML +1.8, DV -7.6 from dura, 10°), and a mixture of AAV-RG and AAV-TVA (1,000 nl of a 1:1 mix) was injected into ipsilateral PL (AP +3.1, ML +1.2, DV -3.8 from skull, 12°). Three weeks later during a second stereotaxic surgery, EnvA-RV-EGFP (1,000 nl) was injected into the same location in ipsilateral PL. Rats were sacrificed 7 days after rabies injections.

Tissue Processing

Rats were deeply anesthetized with isoflurane and then transcardially perfused with 0.9% NaCl followed by 10% neutral-buffered formalin *via* a peristaltic pump (Cole Parmer, Vernon Hills, IL, USA). Brains were collected, post-fixed in 10% formalin overnight at 4°C, placed in 20% sucrose in phosphate-buffered saline (PBS) with 0.02% sodium-azide at 4°C for ≥2 days, frozen in dry ice, cut into 40-μm thick coronal sections on a cryostat, and collected into PBS-azide for storage before immunohistochemistry (IHC). For IHC, all incubations and rinses took place at room temperature on a shaker. Sections were rinsed in PBS three times between steps.

For FG and CTB tracing, free-floating sections were incubated overnight in goat anti-CTB (1:50 K, List Biological Labs Cat# 703, RRID: AB_10013220) in PBS with 0.25% Triton X-100 (PBST, Sigma-Aldrich), and then incubated for 1 h in Alexa Fluor 594-conjugated donkey anti-goat (1:500 in PBST, Jackson Immunoresearch Labs cat# 705-585-147, RRID:AB_2340433). Sections were mounted onto glass slides, coverslipped with ProLong Diamond Antifade (Thermo Fisher Scientific, Fair Lawn, NJ, USA), sealed with clear nail polish, and stored at 4°C.

For RV tracing, one well (every 12th section) was used for mCherry/EGFP fluorescence (for counting starter cells), and one well (every 12th section) was used for IHC to visualize mCherry/EGFP with DAB (for counting inputs to PL). For fluorescence, sections were mounted onto glass slides, coverslipped with ProLong Diamond Antifade, sealed with clear nail polish, and stored at 4°C. For DAB, free-floating sections were incubated for 15 min in 0.3% H₂O₂ in PBS, overnight in mouse anti-DsRed (1:2 K in PBST, Takara Bio Cat# 632392, RRID: AB_2801258), 1 h in biotinylated donkey anti-mouse (1:500 in PBST, Jackson Immunoresearch Labs Cat# 715-065-151, RRID: AB_2340785), and 45 min in ABC (Vector Elite Kit, 1:500 in PBST, Vector). The reaction was visualized *via* incubation for 10 min in 0.025% 3,3'-diaminobenzidine (DAB), 0.05% nickel ammonium sulfate, and 0.015% H₂O₂

(to yield black DAB color). Sections were then incubated overnight in rabbit anti-GFP (1:50 K in PBST, Abcam Cat# ab290, RRID:AB_303395), 1 h in biotinylated donkey anti-rabbit (1:500 in PBST, Jackson Immunoresearch Labs Cat# 711-065-152, RRID: AB_2340593), 45 min in ABC (Vector Elite Kit, 1:500 in PBST, Vector), and visualized *via* the same DAB reaction but without nickel (to yield brown DAB color). Sections were mounted onto Superfrost Plus slides, dried, counterstained with Methyl Green (0.5% in sodium acetate buffer, Sigma-Aldrich), and coverslipped with Permount (Thermo Fisher Scientific, Fair Lawn, NJ, USA).

Data Analysis

Fluorescent and brightfield images were acquired using an Olympus BX51 microscope. For CTB and FG tracing, neurons were counted in PL on two sections per rat. Four rats were excluded from CTB/FG analysis due to small/missing RMTg injections. One rat was removed from CTB/FG analysis after being identified as a significant outlier (Grubb's method) due to a higher percentage of double labeling. The remaining data were analyzed with a paired *t*-test. For rabies tracing, all EGFP-labeled neurons were counted on all sections stained with DAB (every 12th section) and categorized into brain regions according to boundaries identified by Paxinos and Watson (2007). RMTg boundaries were defined (Figures 1B, 2C) according to Smith et al. (2019). A neuron was only counted if a soma was clearly visible. Fluorescent sections were used to count all double-labeled neurons (EGFP + mCherry) on every 12th section.

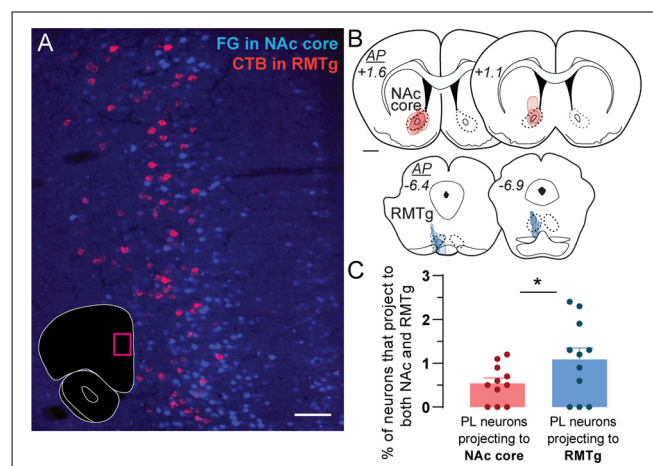
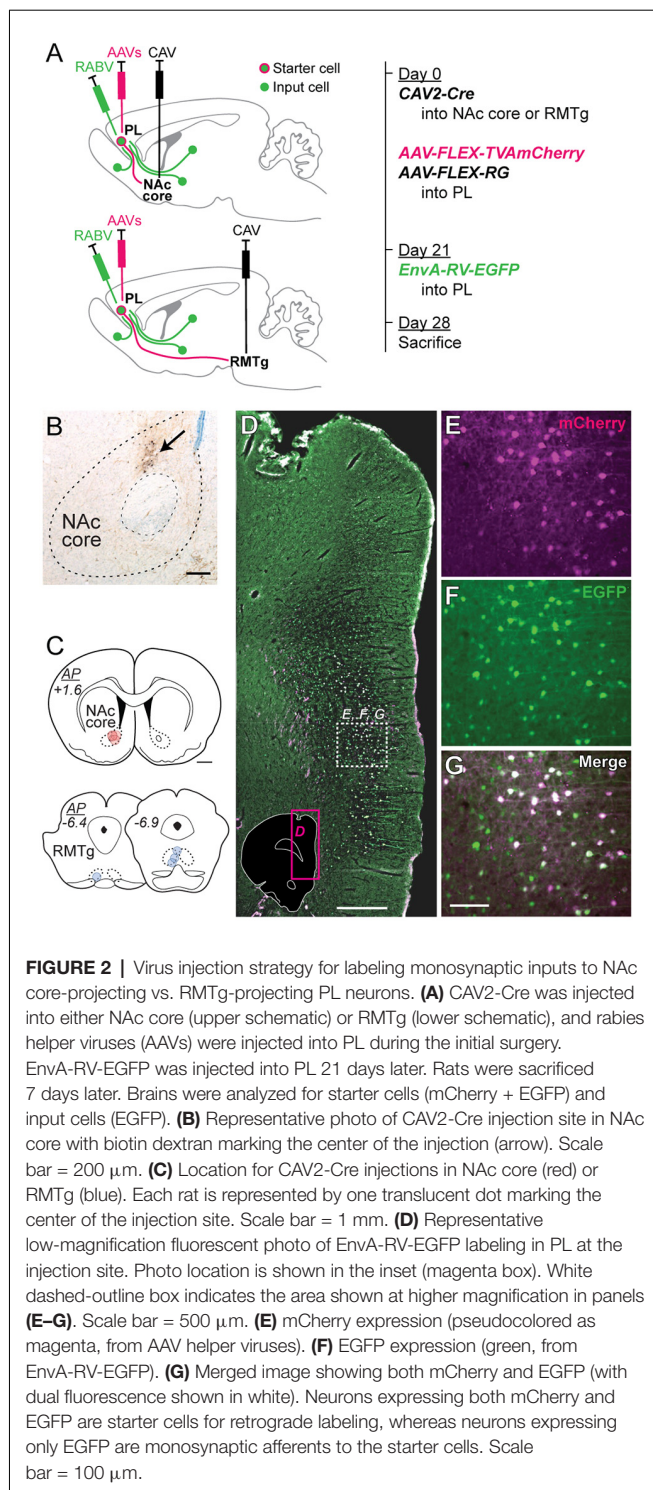


FIGURE 1 | Retrograde tracing of prelimbic (PL) neurons projecting to nucleus accumbens (NAc) core and rostromedial tegmental nucleus (RMTg).

(A) Representative photo of retrogradely-traced neurons in PL following injections of Fluoro-Gold (FG) in NAc core (blue) and CTB in RMTg (magenta). Photo location is shown in the inset (magenta box). Scale bar = 100 μm.

(B) Location and spread for retrograde tracer injections in NAc core (FG, red) and RMTg (CTB, blue). Each rat is represented by one translucent outline, and outlines are overlapped. Anterior-posterior (AP) levels represent mm from bregma. Scale bar = 1 mm.

(C) Percentage of PL neurons that project to both NAc core and RMTg (i.e., double-labeled for both CTB and FG), as a proportion of the total number of PL neurons projecting to NAc core (all FG-labeled cells) or RMTg (all CTB-labeled cells). Averages (± SEM) are shown, as well as individual data points for each rat ($n = 11$, $*p < 0.05$).



Expression of EGFP alone indicated input cells, and expression of both mCherry and EGFP indicated starter cells. Inputs were normalized within each animal and calculated as a percentage of total inputs per rat. Brain regions were only included in analysis and figures if normalized inputs were $\geq 0.2\%$ in ≥ 2 rats. Data were analyzed using two-way ANOVAs (with repeated measures when appropriate) and Sidak *post hoc* analyses.

RESULTS

Conventional Retrograde Tracing in PL Targets

Sparse double labeling was seen in PL (Figure 1A) when conventional retrograde tracers (FG and CTB) were injected into ipsilateral NAc core and RMTg (Figure 1B; $n = 11$). We observed NAc-projecting PL neurons in layers II/III and upper layer V, whereas RMTg-projecting neurons were located in deeper layer V (Figure 1A). Double-labeled neurons (projecting to both NAc core and RMTg) represented only $0.5\% \pm 0.1$ of PL neurons projecting to NAc core and $1.1\% \pm 0.3$ of PL neurons projecting to RMTg (Figure 1C; $t_{(10)} = 3.004$, $p = 0.013$). These data indicate that PL neurons projecting to NAc core vs. RMTg are predominantly separate subpopulations.

Monosynaptic Retrograde Tracing in PL Subpopulations

To determine whether these PL subpopulations differ in terms of input specificity, we conducted monosynaptic retrograde tracing in each projection subpopulation *via* retrograde Cre delivery (Figure 2A). CAV2-Cre was injected into either NAc core ($n = 4$) or RMTg ($n = 4$; Figures 2B,C), and Cre-dependent helper AAVs driving expression of TVA-mCherry and RG were injected into PL. Three weeks later, EnvA-RV-EGFP was injected into PL. Rabies only infects and monosynaptically spreads from neurons expressing both TVA and RG.

We mapped and counted the number of starter cells (mCherry + EGFP) using fluorescent labeling (representative images in Figures 2D–G). We counted the number of input cells (EGFP) across different brain regions using immunohistochemistry with DAB labeling (representative images in Figure 4). Starter cells projecting to either NAc core or RMTg were primarily in PL, but also in neighboring infralimbic cortex (IL; Figure 3A). Although the average number of starter cells differed for NAc vs. RMTg ($t_{(6)} = 5.50$, $p = 0.0015$), the number of transsynaptically labeled cells was correlated with the number of starter cells (Figure 3B; $r = 0.91$, $p = 0.0019$).

Inputs were normalized within each animal and calculated as a percentage of total inputs per rat (Figure 3C). The total ipsilateral inputs were significantly greater than total contralateral inputs (main effect for contra/ipsi: $F_{(1,6)} = 37.354$, $p < 0.0001$), and the two PL subpopulations differed in terms of ipsilateral vs. contralateral inputs (main effect for PL subpopulation: $F_{(1,6)} = 14.24$, $p = 0.009$; interaction: $F_{(1,6)} = 83.43$, $p < 0.0001$). Therefore, we separately analyzed contralateral and ipsilateral inputs when comparing afferents for the two PL subpopulations. PL neurons projecting to NAc core vs. RMTg were significantly different in terms of ipsilateral input (two-way ANOVA, overall effect of PL subpopulation: $F_{(1,6)} = 53.44$, $p = 0.0003$; overall effect of afferents: $F_{(29,174)} = 86.11$, $p < 0.0001$; interaction: $F_{(29,174)} = 5.05$; $p < 0.0001$). We found significant differences for ipsilateral PL and IL (p 's < 0.0001), and mediiodorsal thalamic nucleus (MD; $p = 0.036$). PL neurons projecting to NAc core vs. RMTg were also significantly different in terms of contralateral input (overall effect of PL

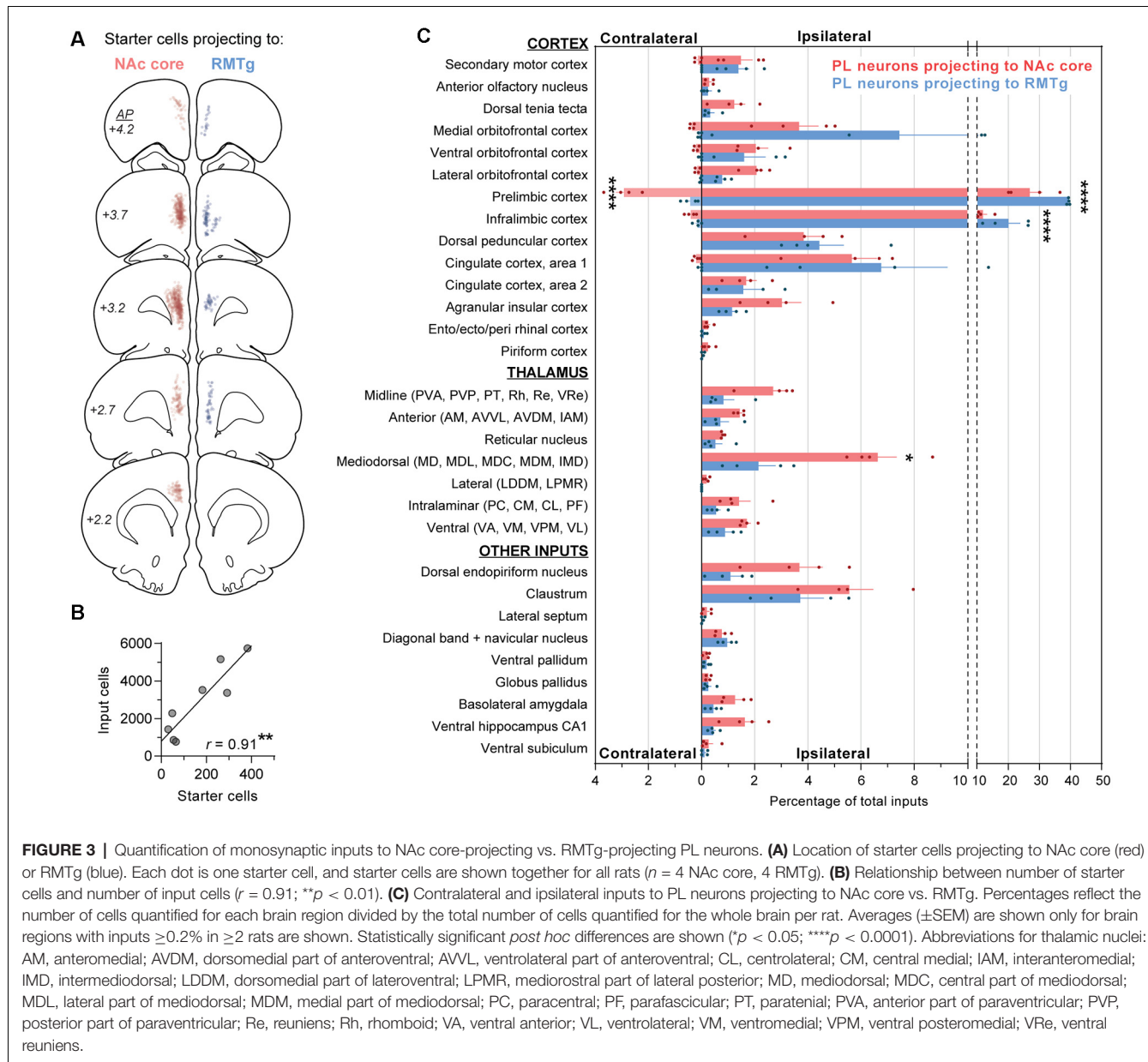
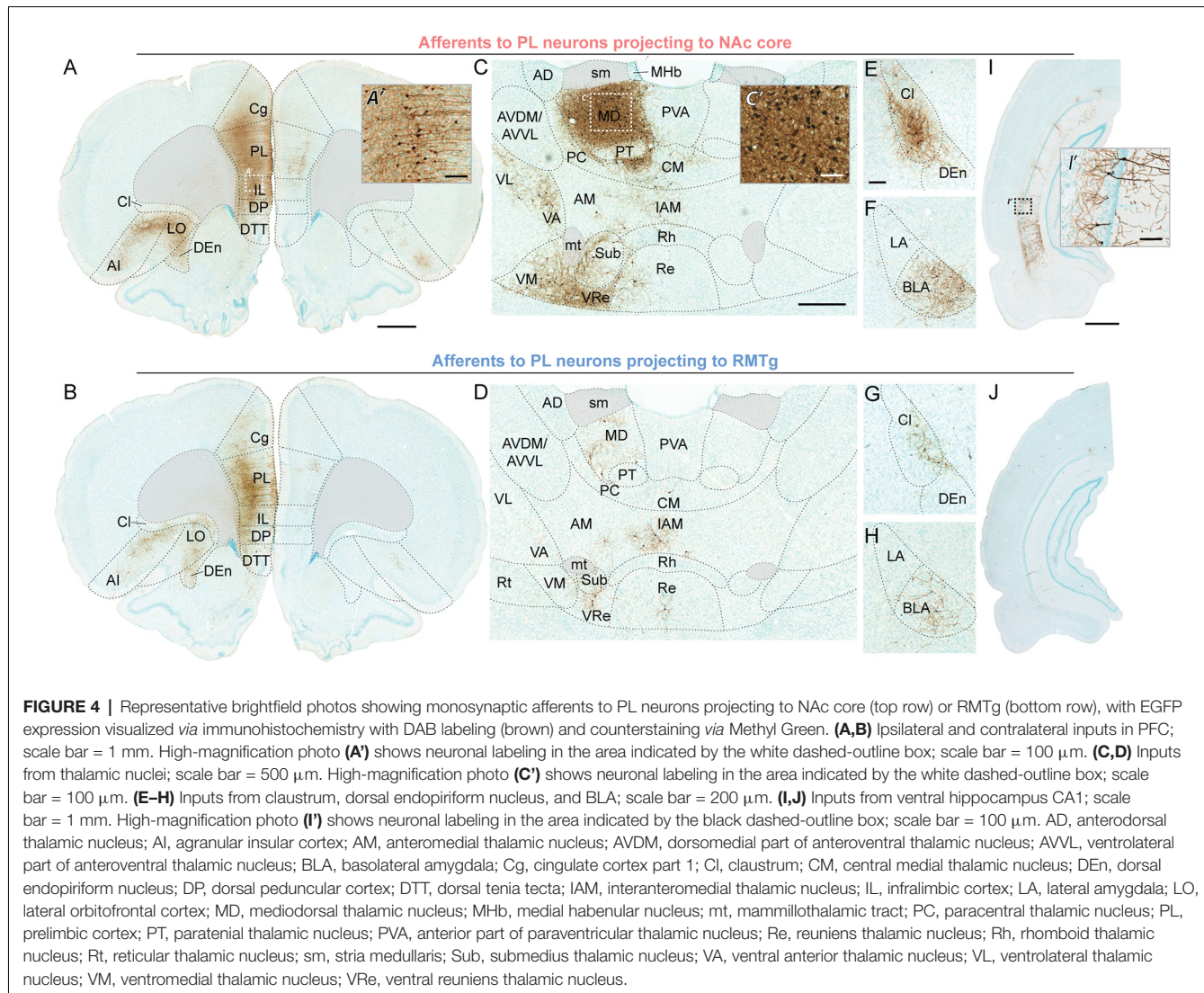


FIGURE 3 | Quantification of monosynaptic inputs to NAc core-projecting vs. RMTg-projecting PL neurons. **(A)** Location of starter cells projecting to NAc core (red) or RMTg (blue). Each dot is one starter cell, and starter cells are shown together for all rats ($n = 4$ NAc core, 4 RMTg). **(B)** Relationship between number of starter cells and number of input cells ($r = 0.91$; $^{**}p < 0.01$). **(C)** Contralateral and ipsilateral inputs to PL neurons projecting to NAc core vs. RMTg. Percentages reflect the number of cells quantified for each brain region divided by the total number of cells quantified for the whole brain per rat. Averages (\pm SEM) are shown only for brain regions with inputs $\geq 0.2\%$ in ≥ 2 rats are shown. Statistically significant post hoc differences are shown (* $p < 0.05$; *** $p < 0.0001$). Abbreviations for thalamic nuclei: AM, anteromedial; AVDM, dorsomedial part of anteroventral; AVVL, ventrolateral part of anteroventral; CL, centrolateral; CM, central medial; IAM, interanteromedial; IMD, intermediodorsal; LDDM, dorsomedial part of lateroventral; LPMR, mediorostral part of lateral posterior; MD, mediodorsal; MDC, central part of mediodorsal; MDL, lateral part of mediodorsal; MDM, medial part of mediodorsal; PC, paracentral; PF, parafascicular; PT, paratenial; PVA, anterior part of paraventricular; PVP, posterior part of paraventricular; Re, reunions; Rh, rhomboid; VA, ventral anterior; VL, ventrolateral; VM, ventromedial; VPM, ventral posteromedial; VRe, ventral reunions.

subpopulation: $F_{(1,6)} = 119.9$, $p < 0.0001$; overall effect of afferents: $F_{(6,36)} = 60.46$, $p < 0.0001$; interaction: $F_{(6,36)} = 34.06$; $p < 0.0001$), with significant differences for contralateral PL ($p < 0.0001$).

For both populations, the primary source of afferent information was neighboring prefrontal neurons in PL and IL (Figures 4A,B). However, RMTg-projecting PL neurons received a significantly higher percentage of inputs from local ipsilateral PL and IL neurons (Figure 3C; PL: $39.4\% \pm 0.2$ and IL: $20.1\% \pm 3.8$), as compared to NAc-projecting PL neurons (PL: $26.9\% \pm 4.0$ and IL: $11.8\% \pm 1.3$). We also observed that RMTg-projecting PL neurons received a higher percentage of input from the medial orbitofrontal cortex (OFC), while NAc-projecting PL neurons received

a higher percentage of input from the dorsal tenia tecta, lateral OFC, and agranular insular cortex. The percentage of inputs was similar for NAc-projecting and RMTg-projecting PL neurons for secondary motor cortex, anterior olfactory nucleus, ventral OFC, dorsal peduncular cortex, cingulate cortex areas 1 and 2, entorhinal/ectorhinal/perirhinal cortex, and piriform cortex. Interestingly, NAc-projecting PL neurons received a significantly greater percentage of contralateral cortical input from PL ($2.92\% \pm 0.30$) as compared to RMTg-projecting PL neurons ($0.43\% \pm 0.15$). NAc-projecting PL neurons also received a greater percentage of contralateral inputs from IL, secondary motor cortex, all areas of OFC (medial, ventral, and lateral), and cingulate cortex area 1.



Both PL subpopulations received prominent afferent information from the thalamus (Figures 4C,D), including subregions within the midline thalamic nuclei (anterior/posterior parts of paraventricular, paratenial, rhomboid, reunions, ventral reunions), anterior thalamic nuclei (anteromedial, ventrolateral/dorsomedial parts of anteroventral, interanteromedial), reticular thalamic nucleus, MD (mediodorsal, lateral/central/medial parts of mediodorsal, intermediodorsal), lateral thalamic nuclei (dorsomedial part of lateroventral, mediorstral part of lateral posterior), intralaminar thalamic nuclei (paracentral, central medial, centrolateral, and parafascicular), and ventral thalamic nuclei (ventral anterior, ventromedial, ventral posteromedial, ventrolateral; Figure 3C). NAc-projecting PL neurons received a higher percentage of inputs from all thalamic regions, as compared to RMTg-projecting PL neurons, with a significant difference observed for MD ($6.6\% \pm 0.7$ vs. $2.1\% \pm 0.6$).

We also saw prominent inputs from the dorsal endopiriform nucleus, claustrum (Figures 4E,G), BLA (Figures 4F,H), and

CA1 in the ventral hippocampus (Figures 4I,J). For all of these areas, NAc-projecting PL neurons received a greater percentage of input (Figure 3C). In contrast, the two subpopulations of PL neurons were similar in terms of afferent input arising from the lateral septum, diagonal band, and navicular nucleus, ventral pallidum, globus pallidus, and ventral subiculum (Figure 3C).

DISCUSSION

We found that PL neurons projecting to NAc vs. RMTg are distinct subpopulations (Figure 1). Pathway-specific monosynaptic retrograde tracing for PL neurons projecting to either NAc vs. RMTg (Figure 2) revealed differences in afferent information to the two PL subpopulations (Figures 3, 4). While RMTg-projecting PL neurons received a greater proportion of inputs from nearby sources in ipsilateral PL and IL, NAc-projecting PL neurons received a greater proportion of inputs from other cortical areas, thalamic nuclei, and subcortical areas. Also, NAc-projecting PL neurons received a

greater proportion of contralateral cortical input. These data are the first to demonstrate anatomical connectivity differences between PL neurons projecting to NAc vs. RMTg, which may contribute to opposing functions of these pathways.

PL Projection Subpopulations

We found very little overlap in PL neuron subpopulations projecting to NAc core vs. RMTg, with NAc-projecting PL neurons located in layers II/III and upper layer V, and RMTg-projecting neurons located in deeper layer V (**Figure 1A**). This corresponds with previous studies using conventional retrograde tracers (e.g., CTB) injected into various mPFC targets, which showed that distinct mPFC neuron subpopulations project to different subcortical targets, including NAc, BLA, MD, lateral hypothalamus, and numerous brainstem areas (Akintunde and Buxton, 1992; Pinto and Sesack, 2000; Gabbott et al., 2005). mPFC neurons in layers II/III, V, and VI have been shown to project to the striatum, while mPFC neurons in layer V project to multiple brainstem targets, including the parabrachial nucleus, periaqueductal gray, ventral tegmental area, dorsal raphe, the nucleus of the solitary tract, and ventrolateral medulla (Pinto and Sesack, 2000; Ding et al., 2001; Gabbott et al., 2005).

Afferent Inputs to PL Subpopulations

Previous studies have mapped afferents to rat PL using conventional retrograde tracers (Condé et al., 1995; Hoover and Vertes, 2007). However, unlike conventional tracers, RV-EGFP allows the separation of starter cells from input cells, so that short-range projections within PL and IL can be assessed. Although previous studies have used RV-EGFP in mouse mPFC, they targeted all projection neurons (Ährlund-Richter et al., 2019), interneuron populations (Ährlund-Richter et al., 2019; Sun et al., 2019), or PL layer V (DeNardo et al., 2015). Here, we used RV-EGFP in rat mPFC and targeted PL neurons projecting to NAc core vs. RMTg to provide more detailed complexity about input specificity to PL subpopulations.

We observed prominent cortical inputs from mPFC (PL, IL, cingulate cortex, secondary motor cortex, dorsal peduncular cortex), OFC (with the highest percentage in medial), and agranular insular cortex, and limited labeling in the anterior olfactory nucleus, dorsal tenia tecta, piriform cortex, and ento/ecto/perirhinal cortex (**Figures 3C, 4A,B**). This parallels previous studies with conventional tracers (Condé et al., 1995; Hoover and Vertes, 2007). We found that for both NAc- and RMTg-projecting populations, the primary source of afferent information was neighboring prefrontal neurons in ipsilateral PL and IL, as shown previously with RV-EGFP targeting layer V neurons in PL (DeNardo et al., 2015). However, we also identified a major distinction between afferent inputs to NAc- and RMTg-projecting neurons. RMTg-projecting PL neurons received a higher percentage of input from ipsilateral PL and IL, as well as medial OFC, but a similar or lower percentage of input from all other cortical areas. In contrast, NAc-projecting PL neurons received a higher percentage of input from ipsilateral dorsal tenia tecta, lateral OFC, and agranular insular cortex. Additionally, NAc-projecting PL neurons received a greater percentage of contralateral input, including from PL,

IL, cingulate cortex area 1, secondary motor cortex, OFC, and dorsal peduncular cortex. These findings indicate that RMTg-projecting neurons may be under greater local control, while NAc-projecting neurons have greater integration of information across hemispheres.

We found that NAc-projecting PL neurons received a higher proportion of inputs from all thalamic regions (**Figures 3C, 4C,D**). We observed the greatest thalamic labeling in MD and moderate labeling in midline thalamic nucleus, as per previous work (Condé et al., 1995; Hoover and Vertes, 2007). We also observed moderate labeling in intralaminar, ventral, anterior, and reticular nuclei, and some labeling in the lateral nucleus (but only in NAc-projecting PL neurons).

For areas outside the cortex and thalamus, we observed prominent labeling in dorsal endopiriform cortex and claustrum, and moderate labeling from ventral hippocampus CA1 and BLA (**Figures 3C, 4E–J**), as described previously (Condé et al., 1995; Hoover and Vertes, 2007; DeNardo et al., 2015). Interestingly, for all of these areas, NAc-projecting PL neurons received a greater percentage of input. Extensive previous work has characterized inputs to both pyramidal neurons and interneurons in PL arising from the ventral hippocampus (Ferino et al., 1987; Jay et al., 1989, 1992; Jay and Witter, 1991; Condé et al., 1995; Carr and Sesack, 1996; Gabbott et al., 2002; Hoover and Vertes, 2007) and BLA (Bacon et al., 1996; Gabbott et al., 2006; Dilgen et al., 2013; Ährlund-Richter et al., 2019). Additionally, we detected afferent information arising from the lateral septum, diagonal band and navicular nucleus, ventral pallidum, globus pallidus, and ventral subiculum. Although previous studies noted some input from lateral and posterior hypothalamus (Condé et al., 1995; Hoover and Vertes, 2007; DeNardo et al., 2015), we observed only sparse labeling (<0.2% in all rats) and thus these areas were excluded from analysis.

Notably, unlike previous studies using conventional retrograde tracers in PL (Condé et al., 1995; Hoover and Vertes, 2007), the current study using RV-EGFP as a tracer did not detect inputs from the monoaminergic nuclei of the brainstem, including ventral tegmental area, dorsal raphe, median raphe, and locus coeruleus, indicating that RV-EGFP does not spread transsynaptically to all retrograde afferent neurons. This is confirmed by previous studies showing a lack of brainstem inputs when using RV-EGFP in PL (DeNardo et al., 2015), and a paucity of dopamine inputs when using RV-EGFP in dorsal striatum as a monosynaptic tracer but not as a traditional retrograde tracer (Wall et al., 2013). These results indicate that the transsynaptic spread of RV-EGFP has reduced efficiency at monoaminergic synapses, possibly due to differences in synapse type, location, or distance, as compared to glutamatergic and GABAergic synapses, and this represents a significant limitation of transsynaptic tracing with RV-EGFP. Alternatively, these data may indicate that these PL subpopulations do not receive direct input from monoamine neurons. However, previous work has shown direct synaptic contact between NAc-projecting mPFC neurons and axon terminals containing tyrosine hydroxylase (Carr et al., 1999). Further studies are needed to determine whether RMTg-projecting PL neurons receive direct synaptic input from monoamine neurons.

Technical Considerations

In this study, we used a two-helper-virus system, and this may have resulted in overestimating starter cells due to the assumption that each cell was successfully infected with both viruses. We did not demonstrate Cre dependence of the helper viruses in the current study (e.g., by including control animals lacking injection of CAV2-Cre), but previous work has shown limited expression of helper viruses in the absence of Cre (Watabe-Uchida et al., 2012; Wall et al., 2013; Schwarz et al., 2015). Additionally, it is important to note that our injections of CAV2-Cre likely were not restricted solely to RMTg, given the small size of RMTg as compared to NAc core and given that many injections show some spread outside the intended target (**Figure 1B**). It is important to note as well that these studies were performed in male rats; future studies are necessary to determine whether sex differences exist for these PL subpopulations. Finally, although RV-EGFP tracing reveals the presence of a connection between two neurons, it does not reveal information about the strength or function of the connection. One neuron may form many synapses onto many neurons and may provide a strong influence despite limited labeling with RV-EGFP. Therefore, additional studies are necessary to explore potential functional differences in afferent input to these PL subpopulations.

Conclusions

The current work shows that PL subpopulations differ not only in their efferent target but also in the proportion of inputs they receive from a variety of afferent structures. When directly compared, RMTg-projecting PL neurons receive a greater proportion of input from nearby cortical input (ipsilateral PL and IL), whereas NAc-projecting PL neurons receive a greater proportion of input from other mPFC and cortical areas, thalamic nuclei, amygdala, and ventral hippocampus, as well as contralateral mPFC. These differences in afferent information may be critical to potential functional differences of these PL subpopulations and may be related to the contrasting roles

REFERENCES

- Ährlund-Richter, S., Xuan, Y., van Lunteren, J. A., Kim, H., Ortiz, C., Pollak-Dorocic, I., et al. (2019). A whole-brain atlas of monosynaptic input targeting four different cell types in the medial prefrontal cortex of the mouse. *Nat. Neurosci.* 22, 657–668. doi: 10.1038/s41593-019-0354-y
- Akintunde, A., and Buxton, D. F. (1992). Origins and collateralization of corticospinal, corticopontine, corticorubral and corticostriatal tracts: a multiple retrograde fluorescent tracing study. *Brain Res.* 586, 208–218. doi: 10.1016/0006-8993(92)91629-s
- Bacon, S. J., Headlam, A. J., Gabbott, P. L., and Smith, A. D. (1996). Amygdala input to medial prefrontal cortex (mPFC) in the rat: a light and electron microscope study. *Brain Res.* 720, 211–219. doi: 10.1016/0006-8993(96)00155-2
- Balcita-Pedacino, J. J., Omelchenko, N., Bell, R., and Sesack, S. R. (2011). The inhibitory influence of the lateral habenula on midbrain dopamine cells: ultrastructural evidence for indirect mediation via the rostromedial mesopontine tegmental nucleus. *J. Comp. Neurol.* 519, 1143–1164. doi: 10.1002/cne.22561
- Barrot, M., Sesack, S. R., Georges, F., Pistis, M., Hong, S., and Jhou, T. C. (2012). Braking dopamine systems: a new GABA master structure for mesolimbic and nigrostriatal functions. *J. Neurosci.* 32, 14094–14101. doi: 10.1523/JNEUROSCI.3370-12.2012
- Bourdy, R., Sánchez-Catalán, M.-J., Kaufling, J., Balcita-Pedacino, J. J., Freund-Mercier, M.-J., Veinante, P., et al. (2014). Control of the nigrostriatal dopamine neuron activity and motor function by the tail of the ventral tegmental area. *NeuroPsychopharmacology* 39, 2788–2798. doi: 10.1038/npp.2014.129
- Callaway, E. M. (2008). Transneuronal circuit tracing with neurotropic viruses. *Curr. Opin. Neurobiol.* 18, 617–623. doi: 10.1016/j.conb.2009.03.007
- Carr, D. B., O'Donnell, P., Card, J. P., and Sesack, S. R. (1999). Dopamine terminals in the rat prefrontal cortex synapse on pyramidal cells that project to the nucleus accumbens. *J. Neurosci.* 19, 11049–11060. doi: 10.1523/JNEUROSCI.19-24-11049.1999
- Carr, D. B., and Sesack, S. R. (1996). Hippocampal afferents to the rat prefrontal cortex: synaptic targets and relation to dopamine terminals. *J. Comp. Neurol.* 369, 1–15. doi: 10.1002/(SICI)1096-9861(19960520)369:1<1::AID-CNE1>3.0.CO;2-7
- Condé, F., Maire-Lepoivre, E., Audinat, E., and Crépel, F. (1995). Afferent connections of the medial frontal cortex of the rat: II. Cortical and subcortical afferents. *J. Comp. Neurol.* 352, 567–593. doi: 10.1002/cne.903520407
- Cruz, A. M., Spencer, H. F., Kim, T. H., Jhou, T. C., and Smith, R. J. (2020). Prelimbic cortical projections to rostromedial tegmental nucleus play a suppressive role in cue-induced reinstatement of cocaine seeking. *NeuroPsychopharmacology* doi: 10.1038/s41386-020-00909-z. [Epub ahead of print].

played by NAc core and RMTg during reward-related behavior, including cocaine seeking. More generally, our data indicate that projection neuron subpopulation may be an important organizational feature of mPFC that has been mostly overlooked, and that differences in afferents, efferents, and function may be critical to the diverse functionality of mPFC across a range of behavioral responses.

DATA AVAILABILITY STATEMENT

The raw data supporting the conclusions of this article will be made available by the authors, without undue reservation.

ETHICS STATEMENT

The animal study was reviewed and approved by the Institutional Animal Care and Use Committee at Texas A&M University.

AUTHOR CONTRIBUTIONS

RS designed the research. AC, TK, and RS performed the research. AC and RS analyzed the data and wrote the article. All authors contributed to the article and approved the submitted version.

FUNDING

This work was supported by National Institutes of Health grant R21 DA037744 (RS).

ACKNOWLEDGMENTS

We thank Thomas Jhou for invaluable discussions and comments on the experimental design and manuscript. We thank Sunila Nair and John Neumaier for providing CAV2-Cre used in pilot experiments for this project.

- DeNardo, L. A., Berns, D. S., DeLoach, K., and Luo, L. (2015). Connectivity of mouse somatosensory and prefrontal cortex examined with trans-synaptic tracing. *Nat. Neurosci.* 18, 1687–1697. doi: 10.1038/nn.4131
- Diehl, M. M., Iravendra-Garcia, J. M., Morán-Sierra, J., Rojas-Bowe, G., Gonzalez-Díaz, F. N., Valentín-Valentín, V. P., et al. (2020). Divergent projections of the prelimbic cortex bidirectionally regulate active avoidance. *eLife* 9:e59281. doi: 10.7554/eLife.59281
- Dilgen, J., Tejeda, H. A., and O'Donnell, P. (2013). Amygdala inputs drive feedforward inhibition in the medial prefrontal cortex. *J. Neurophysiol.* 110, 221–229. doi: 10.1152/jn.00531.2012
- Ding, D. C., Gabbott, P. L., and Totterdell, S. (2001). Differences in the laminar origin of projections from the medial prefrontal cortex to the nucleus accumbens shell and core regions in the rat. *Brain Res.* 917, 81–89. doi: 10.1016/s0006-8993(01)02912-2
- Du Hoffmann, J., and Nicola, S. M. (2014). Dopamine invigorates reward seeking by promoting cue-evoked excitation in the nucleus accumbens. *J. Neurosci.* 34, 14349–14364. doi: 10.1523/JNEUROSCI.3492-14.2014
- Ferino, F., Thierry, A. M., and Glowinski, J. (1987). Anatomical and electrophysiological evidence for a direct projection from Ammon's horn to the medial prefrontal cortex in the rat. *Exp. Brain Res.* 65, 421–426. doi: 10.1007/BF00236315
- Floresco, S. B. (2015). The nucleus accumbens: an interface between cognition, emotion and action. *Annu. Rev. Psychol.* 66, 25–52. doi: 10.1146/annurev-psych-010213-115159
- Gabbott, P., Headlam, A., and Busby, S. (2002). Morphological evidence that CA1 hippocampal afferents monosynaptically innervate PV-containing neurons and NADPH-diaphorase reactive cells in the medial prefrontal cortex (areas 25/32) of the rat. *Brain Res.* 946, 314–322. doi: 10.1016/s0006-8993(02)02487-3
- Gabbott, P. L. A., Warner, T. A., and Busby, S. J. (2006). Amygdala input monosynaptically innervates parvalbumin immunoreactive local circuit neurons in rat medial prefrontal cortex. *Neuroscience* 139, 1039–1048. doi: 10.1016/j.neuroscience.2006.01.026
- Gabbott, P. L. A., Warner, T. A., Jays, P. R. L., Salway, P., and Busby, S. J. (2005). Prefrontal cortex in the rat: projections to subcortical autonomic, motor and limbic centers. *J. Comp. Neurol.* 492, 145–177. doi: 10.1002/cne.20738
- Gourley, S. L., and Taylor, J. R. (2016). Going and stopping: dichotomies in behavioral control by the prefrontal cortex. *Nat. Neurosci.* 19, 656–664. doi: 10.1038/nn.4275
- Hamid, A. A., Pettibone, J. R., Mabrouk, O. S., Hetrick, V. L., Schmidt, R., Vander Weele, C. M., et al. (2016). Mesolimbic dopamine signals the value of work. *Nat. Neurosci.* 19, 117–126. doi: 10.1038/nn.4173
- Hoover, W. B., and Vertes, R. P. (2007). Anatomical analysis of afferent projections to the medial prefrontal cortex in the rat. *Brain Struct. Funct.* 212, 149–179. doi: 10.1007/s00429-007-0150-4
- James, M. H., McGlinchey, E. M., Vattikonda, A., Mahler, S. V., and Aston-Jones, G. (2018). Cued reinstatement of cocaine but not sucrose seeking is dependent on dopamine signaling in prelimbic cortex and is associated with recruitment of prelimbic neurons that project to contralateral nucleus accumbens core. *Int. J. Neuropsychopharmacol.* 21, 89–94. doi: 10.1093/ijnp/pyx107
- Jay, T. M., Glowinski, J., and Thierry, A. M. (1989). Selectivity of the hippocampal projection to the prelimbic area of the prefrontal cortex in the rat. *Brain Res.* 505, 337–340. doi: 10.1016/0006-8993(89)91464-9
- Jay, T. M., Thierry, A.-M., Wiklund, L., and Glowinski, J. (1992). Excitatory amino acid pathway from the hippocampus to the prefrontal cortex. Contribution of AMPA receptors in hippocampo-prefrontal cortex transmission. *Eur. J. Neurosci.* 4, 1285–1295. doi: 10.1111/j.1460-9568.1992.tb00154.x
- Jay, T. M., and Witter, M. P. (1991). Distribution of hippocampal CA1 and subiculum efferents in the prefrontal cortex of the rat studied by means of anterograde transport of Phaseolus vulgaris-leucoagglutinin. *J. Comp. Neurol.* 313, 574–586. doi: 10.1002/cne.903130404
- Jhou, T. C., Fields, H. L., Baxter, M. G., Saper, C. B., and Holland, P. C. (2009a). The rostromedial tegmental nucleus (RMTg), a GABAergic afferent to midbrain dopamine neurons, encodes aversive stimuli and inhibits motor responses. *Neuron* 61, 786–800. doi: 10.1016/j.neuron.2009.02.001
- Jhou, T. C., Geisler, S., Marinelli, M., Degarmo, B. A., and Zahm, D. S. (2009b). The mesopontine rostromedial tegmental nucleus: a structure targeted by the lateral habenula that projects to the ventral tegmental area of Tsai and substantia nigra compacta. *J. Comp. Neurol.* 513, 566–596. doi: 10.1002/cne.21891
- Jhou, T. C., Good, C. H., Rowley, C. S., Xu, S.-P., Wang, H., Burnham, N. W., et al. (2013). Cocaine drives aversive conditioning via delayed activation of dopamine-responsive habenular and midbrain pathways. *J. Neurosci.* 33, 7501–7512. doi: 10.1523/JNEUROSCI.3634-12.2013
- Kaufling, J., Veinante, P., Pawlowski, S. A., Freund-Mercier, M.-J., and Barrot, M. (2009). Afferents to the GABAergic tail of the ventral tegmental area in the rat. *J. Comp. Neurol.* 513, 597–621. doi: 10.1002/cne.21983
- Kaufling, J., Veinante, P., Pawlowski, S. A., Freund-Mercier, M.-J., and Barrot, M. (2010). Gamma-Aminobutyric acid cells with cocaine-induced DeltaFosB in the ventral tegmental area innervate mesolimbic neurons. *Biol. Psychiatry* 67, 88–92. doi: 10.1016/j.biopsych.2009.08.001
- Kremer, E. J., Boutin, S., Chillon, M., and Danos, O. (2000). Canine adenovirus vectors: an alternative for adenovirus-mediated gene transfer. *J. Virol.* 74, 505–512. doi: 10.1128/jvi.74.1.505-512.2000
- Li, H., Pullmann, D., Cho, J. Y., Eid, M., and Jhou, T. C. (2019). Generality and opponency of rostromedial tegmental (RMTg) roles in valence processing. *eLife* 8:e41542. doi: 10.7554/eLife.41542
- McFarland, K., Lapish, C. C., and Kalivas, P. W. (2003). Prefrontal glutamate release into the core of the nucleus accumbens mediates cocaine-induced reinstatement of drug-seeking behavior. *J. Neurosci.* 23, 3531–3537. doi: 10.1523/JNEUROSCI.23-08-03531.2003
- McGlinchey, E. M., James, M. H., Mahler, S. V., Pantazis, C., and Aston-Jones, G. (2016). Prelimbic to accumbens core pathway is recruited in a dopamine-dependent manner to drive cued reinstatement of cocaine seeking. *J. Neurosci.* 36, 8700–8711. doi: 10.1523/JNEUROSCI.1291-15.2016
- Mohebi, A., Pettibone, J. R., Hamid, A. A., Wong, J.-M. T., Vinson, L. T., Patriarchi, T., et al. (2019). Dissociable dopamine dynamics for learning and motivation. *Nature* 570, 65–70. doi: 10.1038/s41586-019-1235-y
- Moorman, D. E., James, M. H., McGlinchey, E. M., and Aston-Jones, G. (2015). Differential roles of medial prefrontal subregions in the regulation of drug seeking. *Brain Res.* 1628, 130–146. doi: 10.1016/j.brainres.2014.12.024
- Otis, J. M., Namboodiri, V. M. K., Matan, A. M., Voets, E. S., Mohorn, E. P., Kosyk, O., et al. (2017). Prefrontal cortex output circuits guide reward seeking through divergent cue encoding. *Nature* 543, 103–107. doi: 10.1038/nature21376
- Paxinos, G., and Watson, C. (2007). *The Rat Brain in Stereotaxic Coordinates*, 6th Edn. San Diego, CA: Academic Press.
- Pinto, A., and Sesack, S. R. (2000). Limited collateralization of neurons in the rat prefrontal cortex that project to the nucleus accumbens. *Neuroscience* 97, 635–642. doi: 10.1016/s0306-4522(00)00042-7
- Schwarz, L. A., Miyamichi, K., Gao, X. J., Beier, K. T., Weissbourd, B., DeLoach, K. E., et al. (2015). Viral-genetic tracing of the input-output organization of a central noradrenaline circuit. *Nature* 524, 88–92. doi: 10.1038/nature14600
- Sicre, M., Meffre, J., Louber, D., and Ambroggi, F. (2019). The nucleus accumbens core is necessary for responding to incentive but not instructive stimuli. *J. Neurosci.* 40, 1332–1343. doi: 10.1523/jneurosci.0194-19.2019
- Smith, R. J., Vento, P. J., Chao, Y. S., Good, C. H., and Jhou, T. C. (2019). Gene expression and neurochemical characterization of the rostromedial tegmental nucleus (RMTg) in rats and mice. *Brain Struct. Funct.* 224, 219–238. doi: 10.1007/s00429-018-1761-7
- Stefanik, M. T., Kupchik, Y. M., and Kalivas, P. W. (2016). Optogenetic inhibition of cortical afferents in the nucleus accumbens simultaneously prevents cue-induced transient synaptic potentiation and cocaine-seeking behavior. *Brain Struct. Funct.* 221, 1681–1689. doi: 10.1007/s00429-015-0997-8
- Stefanik, M. T., Moussawi, K., Kupchik, Y. M., Smith, K. C., Miller, R. L., Huff, M. L., et al. (2013). Optogenetic inhibition of cocaine seeking in rats. *Addict. Biol.* 18, 50–53. doi: 10.1111/j.1369-1600.2012.00479.x
- Sun, Q., Li, X., Ren, M., Zhao, M., Zhong, Q., Ren, Y., et al. (2019). A whole-brain map of long-range inputs to GABAergic interneurons in the mouse medial prefrontal cortex. *Nat. Neurosci.* 22, 1357–1370. doi: 10.1038/s41593-019-0429-9

- Syed, E. C. J., Grima, L. L., Magill, P. J., Bogacz, R., Brown, P., and Walton, M. E. (2016). Action initiation shapes mesolimbic dopamine encoding of future rewards. *Nat. Neurosci.* 19, 34–36. doi: 10.1038/nn.4187
- Vento, P. J., Burnham, N. W., Rowley, C. S., and Jhou, T. C. (2017). Learning from one's mistakes: a dual role for the rostromedial tegmental nucleus in the encoding and expression of punished reward seeking. *Biol. Psychiatry* 81, 1041–1049. doi: 10.1016/j.biopsych.2016.10.018
- Wall, N. R., De La Parra, M., Callaway, E. M., and Kreitzer, A. C. (2013). Differential innervation of direct- and indirect-pathway striatal projection neurons. *Neuron* 79, 347–360. doi: 10.1016/j.neuron.2013.05.014
- Wall, N. R., Wickersham, I. R., Cetin, A., De La Parra, M., and Callaway, E. M. (2010). Monosynaptic circuit tracing *in vivo* through Cre-dependent targeting and complementation of modified rabies virus. *Proc. Natl. Acad. Sci. U.S.A.* 107, 21848–21853. doi: 10.1073/pnas.1011756107
- Warden, M. R., Selimbeyoglu, A., Mirzabekov, J. J., Lo, M., Thompson, K. R., Kim, S.-Y., et al. (2012). A prefrontal cortex-brainstem neuronal projection that controls response to behavioural challenge. *Nature* 492, 428–432. doi: 10.1038/nature11617
- Watabe-Uchida, M., Zhu, L., Ogawa, S. K., Vamanrao, A., and Uchida, N. (2012). Whole-brain mapping of direct inputs to midbrain dopamine neurons. *Neuron* 74, 858–873. doi: 10.1016/j.neuron.2012.03.017
- Wickersham, I. R., Finke, S., Conzelmann, K.-K., and Callaway, E. M. (2007a). Retrograde neuronal tracing with a deletion-mutant rabies virus. *Nat. Methods* 4, 47–49. doi: 10.1038/nmeth999
- Wickersham, I. R., Lyon, D. C., Barnard, R. J. O., Mori, T., Finke, S., Conzelmann, K.-K., et al. (2007b). Monosynaptic restriction of transsynaptic tracing from single, genetically targeted neurons. *Neuron* 53, 639–647. doi: 10.1016/j.neuron.2007.01.033
- Wickersham, I. R., Sullivan, H. A., and Seung, H. S. (2010). Production of glycoprotein-deleted rabies viruses for monosynaptic tracing and high-level gene expression in neurons. *Nat. Protoc.* 5, 595–606. doi: 10.1038/nprot.2009.248

Conflict of Interest: The authors declare that the research was conducted in the absence of any commercial or financial relationships that could be construed as a potential conflict of interest.

Copyright © 2021 Cruz, Kim and Smith. This is an open-access article distributed under the terms of the Creative Commons Attribution License (CC BY). The use, distribution or reproduction in other forums is permitted, provided the original author(s) and the copyright owner(s) are credited and that the original publication in this journal is cited, in accordance with accepted academic practice. No use, distribution or reproduction is permitted which does not comply with these terms.